

ANALYZING THE PDE SOLUTIONS USING OPTICAL FLOW TECHNIQUE: A CASE STUDY WITH 2D HEAT FLOW

Mehmet Önder Efe*

University of Turkish Aeronautical Association
Ankara, Turkey

ABSTRACT

Optical flow technique is one of the powerful motion analysis approach used in computer vision for many purposes. This paper considers the use of optical flow technique to analyze the behavior of Partial Differential Equation (PDE) solutions. Since the flows are solutions of PDEs, whose numerical details may not be precisely available. A video sequence obtained from a thermal camera can be an example to this. The proposed approach lets the engineers interpret how the flow is changing over the physical media. As an illustrative example, we consider 2D heat flow and simulation results have shown that optical flow technique could be utilized in qualitative PDE analysis.

INTRODUCTION

The research on PDEs have been an interesting topic in almost all engineering disciplines as the real world phenomena are governed mostly by PDEs and understanding the nature entails the knowledge on PDEs. Mathematics of PDEs offer very elegant solutions to many cases and the availability of software tools facilitate visualizing the solutions and their temporal change. Almost all engineering disciplines need the knowledge of PDEs and especially in the case of aeronautical and astronautical sciences the importance of the topic is critical. Flexible structures, thermal systems and their interactions, fluids passing over arbitrary geometries are just to name a few of real-world PDE-governed phenomena.

Computer vision with the subfields image and video processing, on the other hand, has lots of powerful tools to understand the cognitive content of an image or video. The development of the high speed computers have made it possible to analyze large amount of real time data and we consider a well-known technique, named optical flow, to understand the time solution of PDEs.

Optical flow is a method that derives the apparent motion of brightness/darkness patterns in an image. The generated flow vector is proportional to the motion of brightness or darkness at a point and the method is effective when the investigated object and the viewer are both moving, [Horn and Schunk , 1980]. Optical flow takes the advantage of gradients of the temporal and spatial information to calculate approximate motion vectors, i.e. the temporal derivatives lead to the detection of motion in time domain, and spatial derivatives facilitate the perception of the motion in the two dimensional (2D) coordinate system, [Barron et al. , 1994]. A number of methods to calculate the optical flow are proposed in the literature. The techniques to determine the optical flow can be categorized as differential methods, correlation based methods and frequency based methods [Barron et al. , 1994]. In frequency based techniques, spatiotemporal velocity-tuned linear filters are utilized to create the new form of the image sequence, and optical flow velocity matrix is obtained from the new form of the image sequence [Fleet and Jepson , 1990]. In the correlation based method, features are extracted from sequential images and optical flow is calculated as a matching feature obtained using the consecutive images [Camus , 1997]. Differential optical flow techniques take the advantage of spatiotemporal derivatives

*Professor of Electrical and Electronics Engineering Department, Email: onderefe@iee.org

of image sequences [Barron et al. , 1994]. Differential-based optical flow algorithms - Lucas-Kanade [Lucas , 1984; Lucas and Kanade , 1981], Horn & Schunk [Horn and Schunk , 1980; Barron et al. , 1994] - have been experimented in the current paper, and due to its prominent features, Horn & Schunk algorithm is chosen to determine the optical flow.

This paper is organized as follows: The second section presents the optical flow technique, the third section describes the 2D heat flow and the numerical issues associated to it. The fourth section considers three experiments, namely, i) 2D heat flow visualization with single sinusoidal excitation and high thermal diffusivity parameter, ii) 2D heat flow visualization with medium thermal diffusivity parameter causing heat waves and sinusoidal excitation, iii) 2D heat flow with arbitrarily chose four excitations and medium thermal diffusivity parameter. The experiments enable the reader to understand the information contained in the optical flow vectors. The fifth section introduces a gray scale augmented optical flow field construction and conclusions are presented at the end of the paper.

COMPUTING THE OPTICAL FLOW

Assuming $I(x, y, t)$ as the gray scale density function (intensity image), if the Taylor series expansion of gray scale density function is evaluated, we obtain the expression in (1).

$$I(x + \delta x, y + \delta y, t + \delta t) = I(x, y, t) + I_x \delta x + I_y \delta y + I_t \delta t + H.O.T. \quad (1)$$

where I_x and I_y are spatial partial derivatives respectively along x , and y directions and I_t stands for the temporal derivation of intensity image with respect to time, and H.O.T. abbreviation is the higher order terms of Taylor series expansion, δx , δy , δt are very small changes in x , y , and t . Higher order terms can be neglected because these terms are small in magnitude, and the equation can be written as in (2), which is indeed an approximation.

$$I(x + \delta x, y + \delta y, t + \delta t) \cong I(x, y, t) + I_x \delta x + I_y \delta y + I_t \delta t \quad (2)$$

Taking the limits $\delta x \rightarrow 0$, $\delta y \rightarrow 0$ and $\delta z \rightarrow 0$ the above expression can be simplified as given below:

$$I_x \frac{dx}{dt} + I_y \frac{dy}{dt} + I_t = 0 \quad (3)$$

If the above expression is rearranged, we get

$$I_t = -(I_x \dot{x} + I_y \dot{y}) \quad (4)$$

where \dot{x} and \dot{y} are the time derivatives of x , and y . Velocity vector in x and y directions can be expressed as

$$V := (u, v) = (\dot{x}, \dot{y}) \quad (5)$$

and and the relationship between I_x , I_y , velocities and I_t are stated compactly in (6). Since the image domain is quantized, the necessary derivatives such as I_x , I_y and I_t can be computed numerically. With these definitions, we have

$$I_t = -(I_x u + I_y v) \quad (6)$$

$$= -\nabla I \cdot V \quad (7)$$

Velocities in x and y directions (u, v) will be computed using iterative methods as there is only one equation but two unknowns (u, v) . Horn and Schunck suggest loose classification technique which minimizes the general error and the noise error to solve this problem, [Horn and Schunk , 1980]. Partial derivatives can be calculated as given as in (8)-(10), and axial indexing to calculate them is shown in Figure 1.

$$I_x \approx \frac{1}{4} (I_{i,j+1,k} - I_{i,j,k} + I_{i+1,j+1,k} - I_{i+1,j,k} + I_{i,j+1,k+1} - I_{i,j,k+1} + I_{i+1,j+1,k+1} - I_{i+1,j,k+1}) \quad (8)$$

$$I_y \approx \frac{1}{4} (I_{i+1,j,k} - I_{i,j,k} + I_{i+1,j+1,k} - I_{i,j+1,k} + I_{i+1,j,k+1} - I_{i,j,k+1} + I_{i+1,j+1,k+1} - I_{i,j+1,k+1}) \quad (9)$$

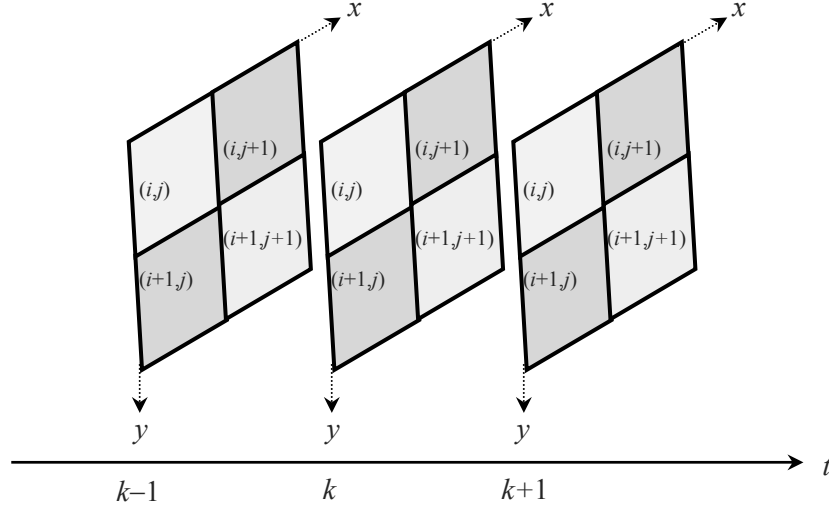


Figure 1: Matrix which is used for calculating gradients x , y directions and time domain (k and $k + 1$ are consecutive solutions of the PDE)

$$I_t \approx \frac{1}{4} (I_{i,j,k+1} - I_{i,j,k} + I_{i+1,j,k+1} - I_{i+1,j,k} + I_{i,j+1,k+1} - I_{i,j+1,k} + I_{i+1,j+1,k+1} - I_{i+1,j+1,k}) \quad (10)$$

where $I_{i,j,k}$ is gray scale density function for i -th row j -th column and k -th temporal frame. i , j , and k index the entries in y , x and time directions, respectively. In order to determine the optical flow vectors accurately, illumination changes should be minimized using the smoothness measure given by (11), which is desired to be close to zero.

$$J_s^2 := \left(\frac{\partial u}{\partial x} \right)^2 + \left(\frac{\partial u}{\partial y} \right)^2 + \left(\frac{\partial v}{\partial x} \right)^2 + \left(\frac{\partial v}{\partial y} \right)^2 \quad (11)$$

On the other hand, we also would like to maintain the below quantity around zero. This practically implies the minimization of the cost functional in (13).

$$J_b = I_t + \nabla I \cdot V \quad (12)$$

$$J = \iint_{\Omega} (\alpha^2 J_s^2 + J_b^2) dx dy \quad (13)$$

where $\alpha > 0$ is a coefficient determining the relative importance of the terms contributing to the total cost defined over the image domain Ω . Defining $\mu(u)$ and $\mu(v)$ as the approximate Laplacians of the velocity components u and v , respectively, and using the calculus of variation for (13), we arrive at the following equations, which we can solve for u and v iteratively.

$$(\alpha^2 + I_x^2 + I_y^2) u = (\alpha^2 + I_y^2) \mu(u) - I_x I_y \mu(v) - I_x I_t \quad (14)$$

$$(\alpha^2 + I_x^2 + I_y^2) v = -I_x I_y \mu(u) + (\alpha^2 + I_x^2) \mu(v) - I_y I_t \quad (15)$$

Assuming velocity estimate for n -th frame as (u^n, v^n) , and $(n + 1)$ -th frame as (u^{n+1}, v^{n+1}) ; velocities are computed using (16) and (17), iteratively.

$$u^{n+1} = \mu(u^n) - I_x \frac{I_x \mu(u^n) + I_y \mu(v^n) + I_t}{\alpha^2 + I_x^2 + I_y^2} \quad (16)$$

$$v^{n+1} = \mu(v^n) - I_y \frac{I_x \mu(u^n) + I_y \mu(v^n) + I_t}{\alpha^2 + I_x^2 + I_y^2} \quad (17)$$

The aforementioned process yields two velocity matrices having the same size with intensity image, say u and v , and the obtained velocity matrices will be used for obstacle avoidance and turn detection processes. For an in depth discussion of the Horn & Schunck method, the reader is referred to Horn and Schunk [1980].

2D HEAT FLOW

2D heat flow process is governed by the PDE given as

$$\frac{\partial w(x, y, t)}{\partial t} = c^2 \left(\frac{\partial^2 w(x, y, t)}{\partial x^2} + \frac{\partial^2 w(x, y, t)}{\partial y^2} \right) \quad (18)$$

where $c > 0$ denotes the thermal diffusivity constant. The physical domain of the process is a square defined as $\Omega := \{(x, y) | 0 \leq x \leq 1, 0 \leq y \leq 1\}$. The initial conditions for all cases considered in this paper are zero, i.e. $w(x, y, 0) = 0$ and boundary conditions are Dirichlet type. We consider $w(0, 0, t)$, $w(0, 1, t)$, $w(1, 0, t)$ and $w(1, 1, t)$ as independently specified external signals and once specified the quadruple, the outer solutions $w(0, y, t)$, $w(1, y, t)$, $w(x, 0, t)$ and $w(x, 1, t)$ are constructed using Crank-Nicholson implicit scheme. After that, the interior matrix is computed again by utilizing the Crank-Nicholson implicit scheme.

In constructing the numerical solution, we set a linear grid having $N_x = N_y = 25$ grid points in each axis. This means $\Delta x = \frac{1}{N_x - 1}$ and $\Delta y = \frac{1}{N_y - 1}$ and the discretized domain of the 2D heat flow problem is denoted by $\Omega_d := \{(x_k, y_l) | x_k = k\Delta x, y_l = l\Delta y\}$ with $k = 1, 2, \dots, N_x, l = 1, 2, \dots, N_y$.

Looking at the temporal axis, we chose $\Delta t = 5$ milliseconds in obtaining the numerical values and the end time of the solver is set $T = 2$ seconds. Basically, the whole course of the numerical side consists of 401 snapshots, the first of which is the zero initial conditions.

OPTICAL FLOW BASED ANALYSIS OF THE PDE SOLUTION

In this section, we consider three cases and interpret the vector fields generated by the optical flow technique. In doing this, we set picture depth to 2, which means that 2 pictures are involved in computing the instantaneous optical flow field, and we iterate the optical flow computation 10 times to obtain an accurate picture of how it spreads over Ω_d .

First Case

In this experiment, we investigate a process with thermal diffusivity constant $c = 3$ and $w(0, 0, t) = \sin(\pi t)$. The BCs at other three corners are zero. The process is highly diffusive as the thermal diffusivity constant is relatively large. The results obtained are illustrated in Figure 2. The figure has three columns. The leftmost column illustrates the instantaneous solutions for the value of $w(0, 0, t)$ shown in the middle column, where we mark the value of the BC exactly at the instant of snapshot shown on the left. The rightmost column depict the obtained optical flow vector. Since we have the numerical values with full details, we also depict the contours to understand the optical flow better.

Figure 2 has four rows. First row depicts the results observed when $t = 0.25$ sec., the second row is for $t = 0.75$ sec., the third row is for $t = 1.25$ sec. and the last row is for $t = 1.75$ sec. Since the process is highly diffusive, the BC at $w(0, 0, t)$ is the visible maximum/minimum point. This is evident from the optical flow fields as the flow is outward when $|w(0, 0, t)|$ is increasing, and it is inward when $|w(0, 0, t)|$ is decreasing. From an image processing point of view, this observation can be explained as follows: When $|w(0, 0, t)|$ is increasing, the brighter/darker pixels are in the radially outward direction and the flow is in the outward direction. This is evident from the optical flow fields in the 1st and 3rd rows. When $|w(0, 0, t)|$ is decreasing, brighter/darker pixels are in the radially inward direction and optical flow field is pointing toward the (0,0) corner as seen from the 2nd and 4th rows of Figure 2.

This setting is simple as it does not produce peaks and interestingly, it distinguishes the diffusing effect regardless of its physical outcome like heating or cooling.

Second Case

In this case, we repeat the first experiment with $c = 0.7$ and obtain the results shown in Figure 3. To better visualize the behavior, we change the observation instants to 0.5 sec., 1 sec, 1.5 sec and 2 sec. The results seen in the first row are similar to those we saw in Figure 2. Same can be said for the third row as the full solutions displays a dominant BC influencing the entire flow field and the optical flow is consistently in the outward direction. What differs is the following: In the 2nd row of Figure 3, we see a temporally local maximum other than the BC and in the 4th row, we see a local minimum other than the BC. This phenomenon creates a contour line, on which the optical flow vector magnitudes are zero, and at the sides of it, the optical flow is

toward the contour. The contour of zero optical flow magnitude vectors is moving and basically this shows us that the optical flow identifies the direction of change. The change may be the diffusion of darker pixels or brighter pixels.

Third Case

In the third experiment, we consider the 2D heat flow with $c = 0.7$ and all four corners have nonzero Dirichlet type boundary conditions given in (19)-(22).

$$w(0, 0, t) = \sin(\pi t) \quad (19)$$

$$w(0, 1, t) = \sin(2\pi t) \quad (20)$$

$$w(1, 0, t) = \sin(2\pi t/3) \quad (21)$$

$$w(1, 1, t) = \sin(2\pi t/5) \quad (22)$$

For this experiment, the change of the optical flow field is fast and we produce four figures to study it. In Figure 4, the snapshots for $t \in \{0.125, 0.25, 0.375, 0.5\}$ instants are shown. Same is repeated in Figure 5 for $t \in \{0.625, 0.75, 0.875, 1\}$ instants and so on for Figures 6-7.

In Figure 4, the four boundary values are increasing and the optical flow field is pointing toward the interior of Ω_d . In this figure, BCs elevate the solution surface and in Figure 5, we see changes in flow directions. This change becomes highly visible in Figure 6 such that higher corners push brighter pixels while lower corners push darker pixels. The bottom row of Figure 6 shows that the BC at $(x, y) = (0, 0)$ is dominantly forcing the flow of darker pixels. Same is evident from the top three rows of Figure 7, and we see radical differences in the bottom row of Figure 7. Since the solution displays fast changes occurring over the physical domain of the process, we present many figures to interpolate what happened in between two consecutive rows. Optical flow mainly detects where the change is occurring and puts a vector whose magnitude is proportional to the change at that particular location. In what follows, we consider how we can improve the technique to increase its understandability.

GRAY LEVEL AUGMENTED OPTICAL FLOW TO VISUALIZE HEAT TRANSPORT

Clearly the bipolar nature of the optical flow technique makes it difficult to interpret the flow vectors, which are changing fast. This is basically because the technique does not distinguish the flow of warming or cooling effects. More explicitly, the flow vectors point the same direction if the corner condition is getting away from zero regardless of its sign. To alleviate this problem, we augment the optical flow with the gray level picture. Let the optical flow vector at a point (x, y) be given by (u, v) . Choose the vertical component of the optical flow as given in (23).

$$p := \gamma \frac{(I(x, y) - 128)}{128} \quad (23)$$

where $0 \leq I(x, y) \leq 255$ is the gray level, and $\gamma := \sqrt{g_x^2 + g_y^2}$ with g_x and g_y being the optical flow grid size in x and y directions, respectively. Such a choice prevents the dominance of $\frac{(I(x, y) - 128)}{128}$ term over u and v , and makes it visible to see the flow vectors better. An example is shown in Figure 8, where we redraw the results of the third experiment. The magnitude for the diffusion of brighter pixels is now with positive p component while that of darker pixels is with negative p component. In Figure 8, the results for $t \in \{0.25, 0.75, 1.25, 1.75\}$ sec. are shown. Just to increase the understandability, the contours are also drawn. Briefly;

- Compare the top left subplot with the rightmost subplot in the second row of Figure 4. p component of the optical flow field is positive over Ω_d .
- Compare the top right subplot with the rightmost subplot in the second row of Figure 5. Propagation of darker pixels is visible here. The vectors erect from downward direction to upward direction. When the gray level is 128, the vectors are in the horizontal plane with zero p component.
- Compare the bottom left subplot with the rightmost subplot in the second row of Figure 6. This figure is the snapshot of $t = 1.25$ sec. and we see that pixel corresponding to $(x, y) = (0, 0)$ corner is locally pulling the optical flow field below the horizontal plane yet the opposite corner, $(x, y) = (1, 1)$ (or x index and y index equal 25), is dominantly raising the optical flow field upwards.

- Finally, compare the bottom right subplot with the rightmost subplot in the second row of Figure 7. This 3D representation clearly shows how the flow field is affected from the gray level of the obtained image.

The above comparisons let us visualize the motion of change in a heat flow problem. Optical flow is insensitive to the sign of quantities, therefore flow of brighter pixels and darker pixels create the same result. Adding a third dimension and augmenting the optical flow field with the gray scale makes it easier to visualize flows.

CONCLUSIONS

Tools of computer science, especially those in image and video processing have potential use in the analysis of PDEs and real world phenomena. Optical flow technique is one of such techniques used in scene analysis and motion estimation. The input to this technique is a video stream and the output is a set of vectors pointing toward the change direction. This paper considers the heat flow as the test PDE as it is easy to understand the mathematics lying behind and interpret the solutions. The 2D case is analyzed and it is seen that the optical flow technique does not distinguish the sign of the local solution. Values getting away from zero produce the same optical flow field. To alleviate this problem, we present a gray level augmented flow field to visualize the flow. This generates a flow field, whose horizontal plane projection is the standard 2D components, yet the vertical component is proportional to the gray level of the image. With such an augmentation, it becomes possible to perform measurements without physically disturbing the thermal process. A thermal camera image would be sufficient to derive such figures.

The proposed visualization method could be extended to fluid flows, cloud motions, vortices in drains and so on. The developer should note that optical flow does not detect the flow of particles in a real line or synthetic phenomenon. The technique detects the change directions based solely on images. Therefore the produced output will be the estimates of the bright and dark pixels as detailed throughout the paper.

ACKNOWLEDGMENTS

Support of Ankara's Development Agency is gratefully acknowledged. The author thanks Dr. Mustafa Kaya, Nevrez İmamoglu and Aydın Eresen for fruitful discussions.

References

- Horn, B.K.P. and Schunck, B.G. (1992). *Determining optical flow*. Artificial Intelligence, 17, p:185-204.
- Barron, J.L., Fleet, D.J. and Beauchemin, S.S. (1994). *Performance of optical flow techniques*. International Journal of Computer Vision, 12(1), p:43-77.
- Fleet, D.J. and Jepson, A.D. (1990). *Computation of component image velocity from local phase information*. International Journal of Computer Vision, 5(1), p:77-104.
- Camus, T.A. (1997). *Real-time quantized optical flow*. The Journal of Real-Time Imaging, 3, p:71-86.
- Lucas, B.D. (1984). *Generalized image matching by the method of differences*. Ph.D. Thesis, Carnegie-Mellon University.
- Lucas, B. and Kanade, T. (1981). *An iterative image registration technique with an application to stereo vision*. Proceedings of Imaging Understanding Workshop, p:121-130.

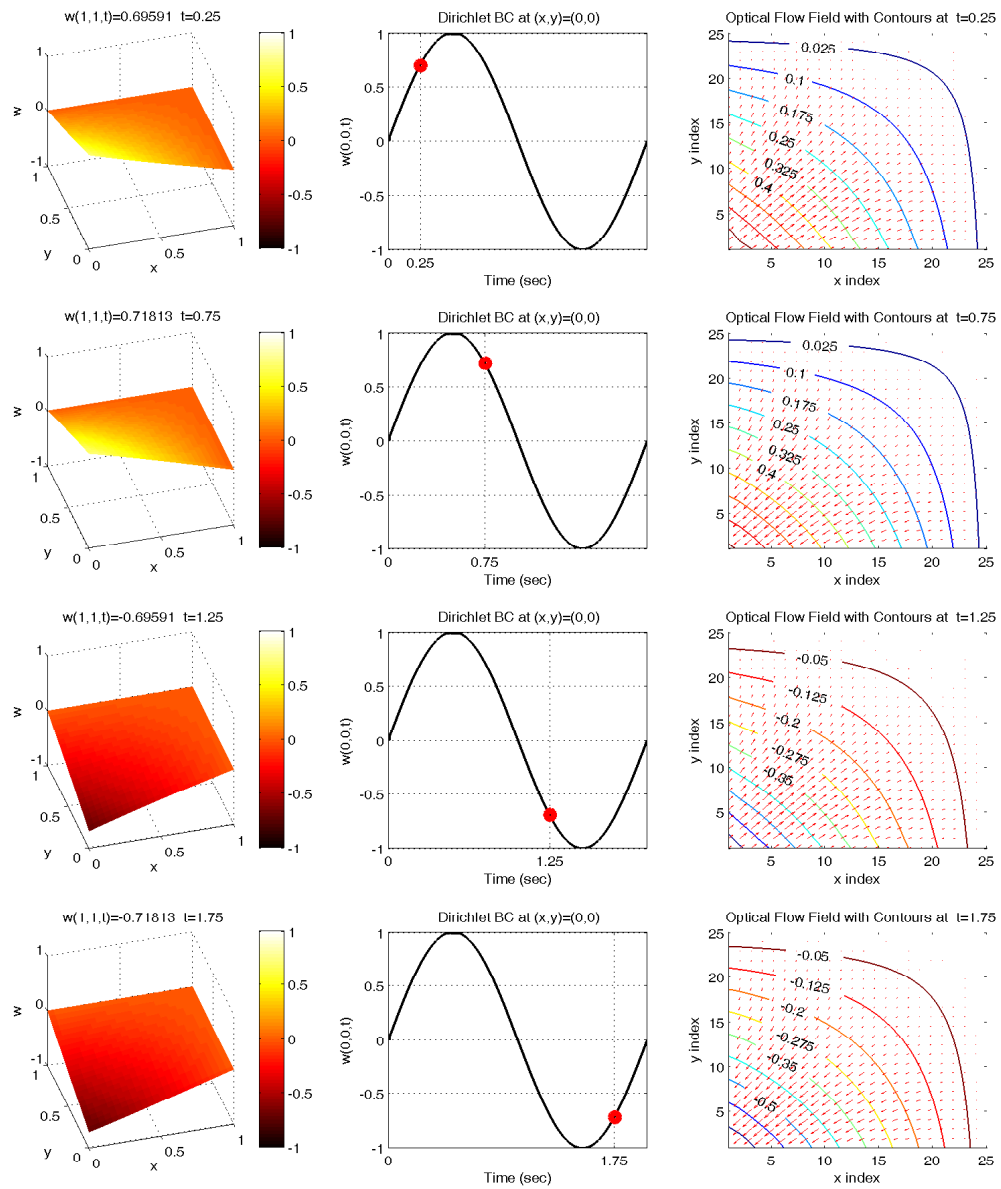


Figure 2: Results of the first experiment. Flow vectors point the diffusion direction of heat flow.

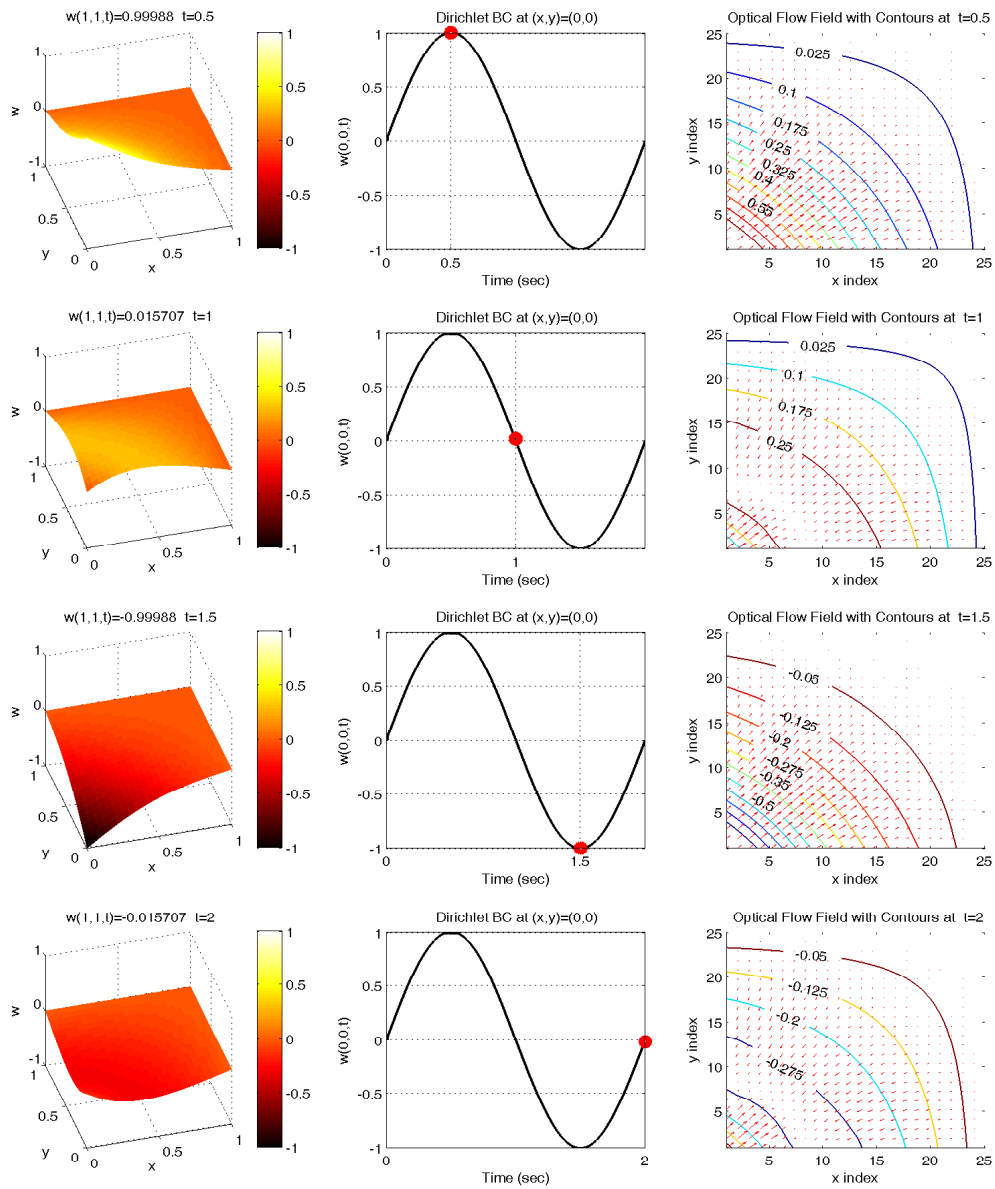


Figure 3: Results of the second experiment. Flow vectors point the diffusion direction of heat flow.

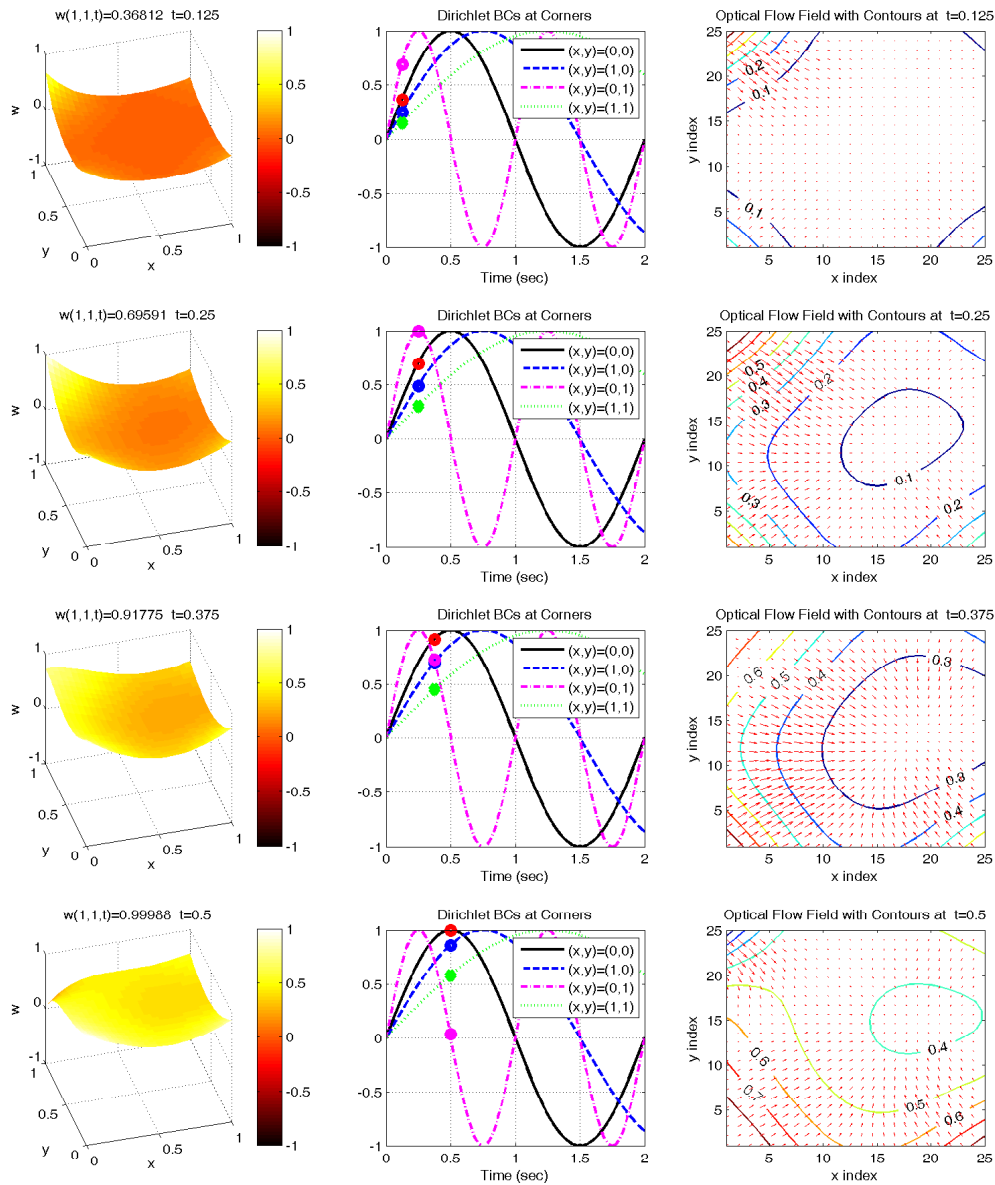


Figure 4: Results of the third experiment for 1st period. Flow vectors point the diffusion direction of heat flow.

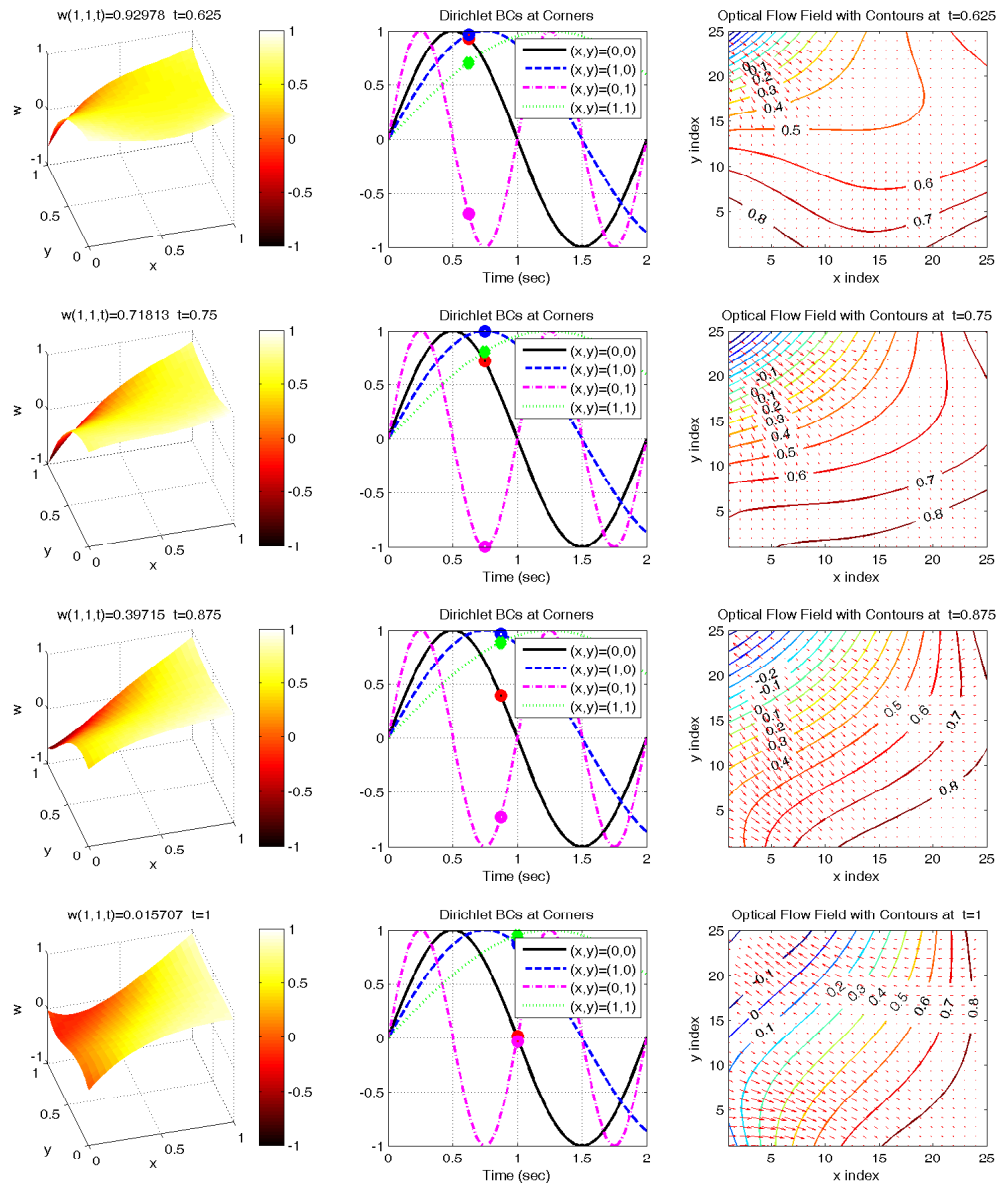


Figure 5: Results of the third experiment for 2nd period. Flow vectors point the diffusion direction of heat flow.

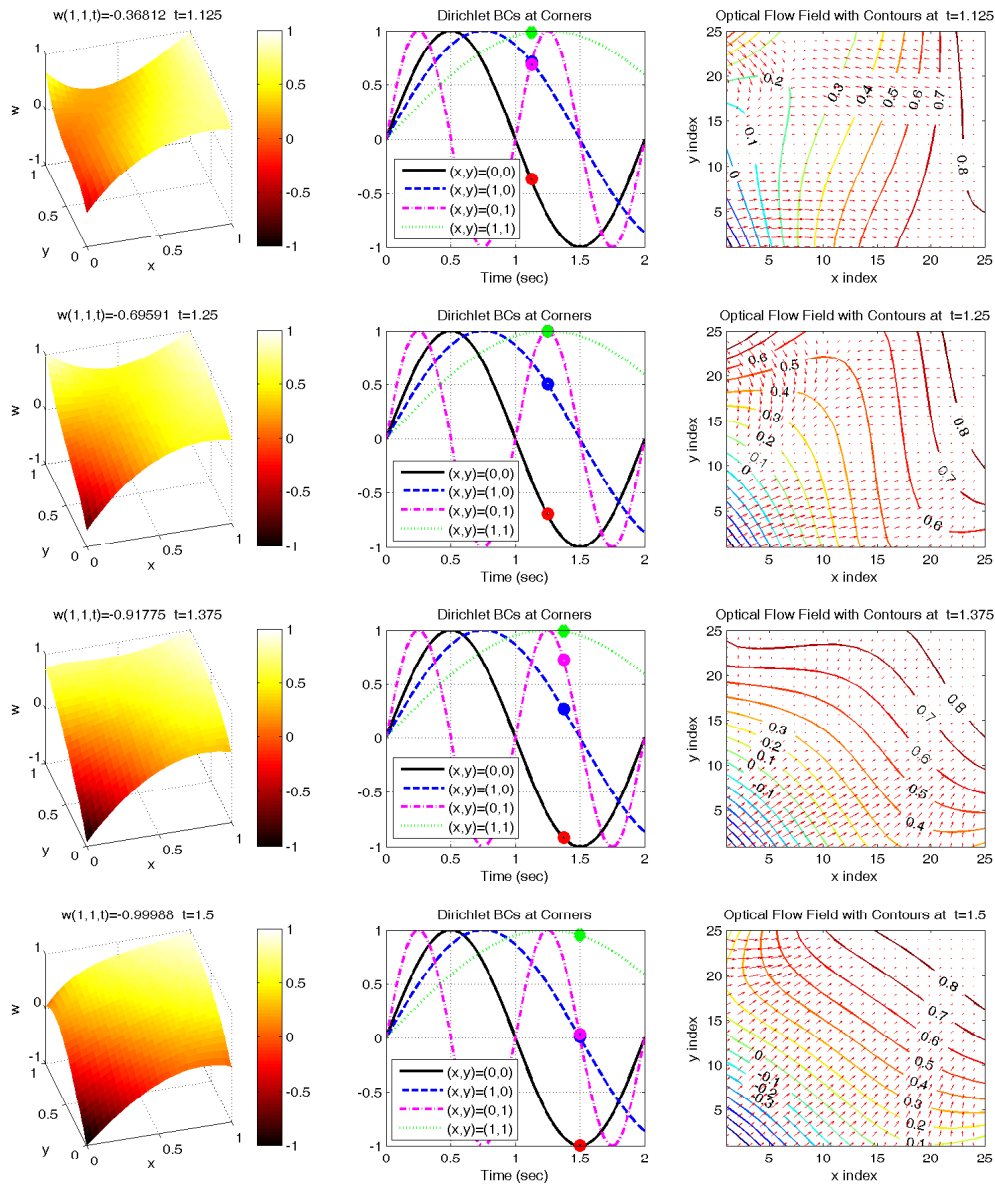


Figure 6: Results of the third experiment for 3rd period. Flow vectors point the diffusion direction of heat flow.

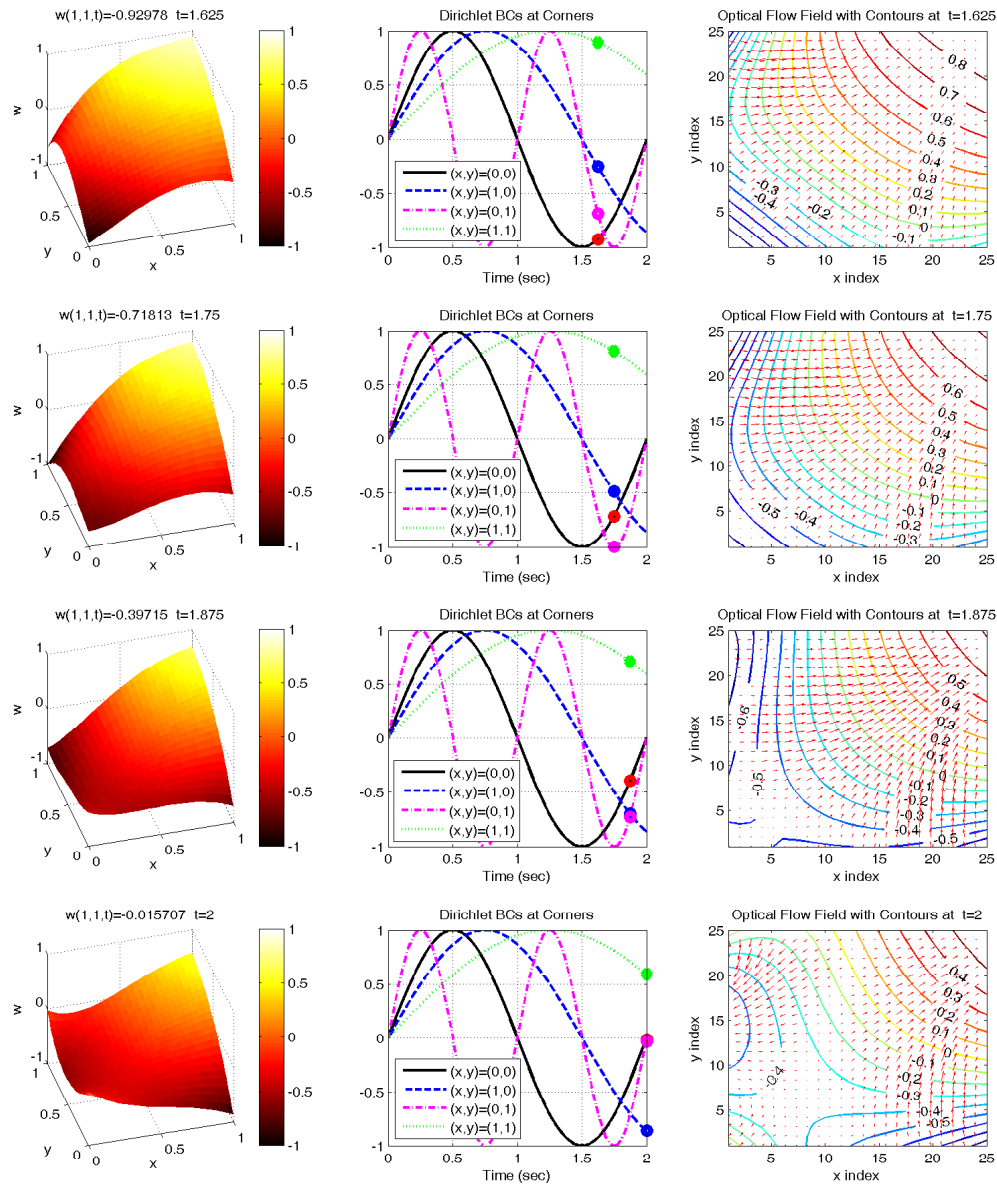


Figure 7: Results of the third experiment for 4th period. Flow vectors point the diffusion direction of heat flow.

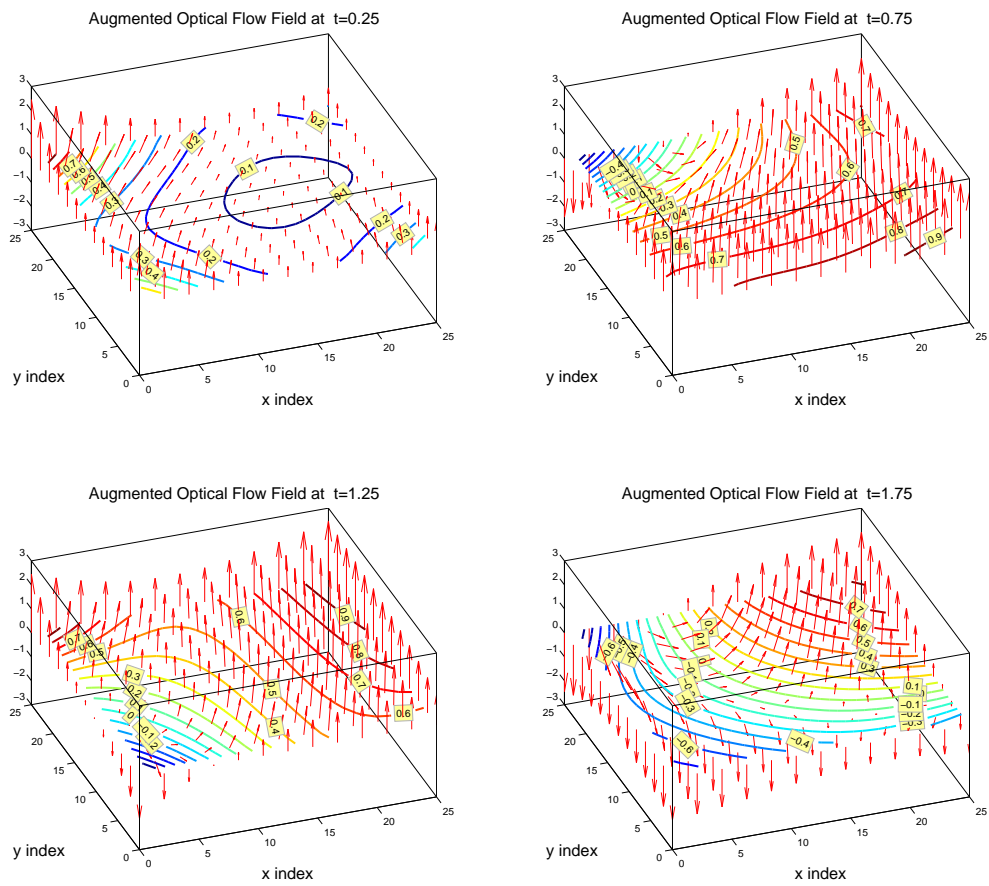


Figure 8: Results of the third experiment for with 3D optical flow discriminating increasing and decreasing heat flow effects